



# AN EMPIRICAL RELATIONSHIP FOR ESTIMATING METALLURGICAL AND MECHANICAL BEHAVIOR OF RESISTANCE SPOT WELDED DP800 STEEL JOINTS

<https://doi.org/10.37255/jme.v4i2pp066-070>

Rajarajan C<sup>1\*</sup>, Sivaraj P<sup>2</sup>, Balasubramanian V<sup>3</sup>

<sup>1</sup>Research scholar, <sup>2</sup>Assistant professor, <sup>3</sup>Professor and <sup>4</sup>Assistant professor

<sup>1-3</sup>Centre for Materials Joining and Research (CEMAJOR), Department of Manufacturing Engineering, Annamalai University, Annamalai Nagar - 608 002.

## ABSTRACT

Similar joints of DP800 (Dual Phase) steel in lap joint configuration were fabricated using resistance spot welding (RSW) process. The process parameters were optimized using DOE (design of experiments) and the welds joints were fabricated using the obtained DOE matrix. The tensile shear fracture load (TSFL) of joints was evaluated using universal testing machine. Microhardness variations across the weld cross-section was recorded using Vickers's microhardness tester. Microstructural features were analyzed using optical microscopy (OM) and scanning electron microscopy (SEM). From this investigation, it is understood that increase in welding current increases the nugget zone size and it led to increasing the decrease of softening in the HAZ. The tensile shear strength is found to increase with increase in welding current up to a certain limit and then it decreases. The microhardness profile shows a peak hardness in nugget zone and the hardness is lower in the HAZ. The softening of HAZ is mainly attributed to inter-critical heating during welding.

**Keywords:** DP steel, Resistance spot welding, Tensile shear fracture, Microstructures

## 1. Introduction

Electrical resistance spot welding one of the prominent sheet metal welding processes automotive industry. In electric resistance spot welding, the overlapping work is positioned between the water-cooled electrodes, and then the heat is obtained by passing a large electrical current for a short period of time [1]. Resistance spot welding is a widely used joining process for fabricating sheet metal assemblies such as automobiles, truck cabins, rail vehicles and home applications due to its advantages in welding efficiency and suitability for automation [2]. For example, a modern auto-body assembly needs 7000 to 12,000 spots of welding according to the size of a car, so the spot welding is an important process in auto-body assembly [1]. Each spot welding is not performed on the same condition because of the alignment of sheets and electrodes as well as the surface condition. For that reason, a spot-welding process needs the optimum process condition that can afford allowance in parametric values for good quality of welding. The optimum condition has to consider There are many factors that affect weld quality, such as voltage fluctuation, electrode misalignment, these actors do not change with weld numbers increasing and can be well controlled through better welding controller or machine maintenance. Advanced high-strength steels for automotive applications have been the aim of research

and the development in recent years. Their introduction in car bodies allows to reduce their weight and improve car safety. Nevertheless, the weldability of AHSS is an important issue since cars typically contain thousands of spot welds [5-8]. Ferrite-martensite dual-phase (DP) steels are some of the most common AHSSs,

From the literature review, it is understood that a lot of research work carried out on DP 600 steels, but very limited work carried on DP 800 steels. Hence, in this investigation, an attempt has been made to understand the developed an empirical relationship for estimating metallurgical and mechanical behavior of resistance spot welded DP800 steel joints.

## 2. Experimental Details

### 2.1 Material Characterization

The material used in this study, supplied by Kaizen cold formed Steel, is cold rolled a galvanized sheet of DP800 steel with 1.6 mm thickness. As can be seen from the chemical composition listed in Table 1 and the mechanical properties of base metals are shown in Table 2 respectively,

The material is low carbon steel, with additions of a relatively high level of manganese, plus some Si and Cr to facilitate the formation of the dual phase microstructure and to offer the aimed properties.

\*Corresponding Author - E- mail: rajachozhan93@gmail.com

Figure 1 shows the initial microstructures consisted of 85% ferrite and 15% martensite. The average ferrite grain size was 7  $\mu\text{m}$ .

**Table 1 chemical composition (wt%) base metal**

C	Si	Mn	Cr	P	S	Ni	Mo	Ti
0.146	0.88	1.500	0.025	0.007	0.0036	0.027	0.0018	0.0016

**Table 2 Mechanical properties of the base metal**

Material	0.2% offset Yield Strength (MPa)	Ultimate Tensile Strength (MPa)	Elongation in 50 mm gauge length (%)	Microhardness (HV)
DP steel	604	812	26	295

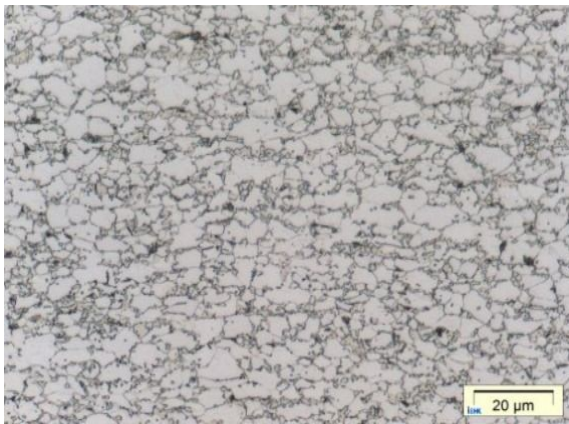


**Fig. 1 Optical micrograph of the base material**

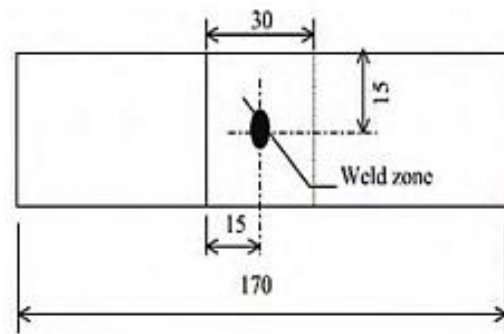
**2.2 Optimizing the Resistance Spot Welding Process Parameters**

The response surface methodology (RSM) was used to optimize the parameters in this study. RSM is a collection of mathematical and statistical techniques that are useful for designing a set of experiments, developing a mathematical model, analyzing the optimum combination of input parameters, and expressing the values graphically. To obtain the influencing nature and optimized condition of the process on tensile shear fracture load and cross tensile fracture load.

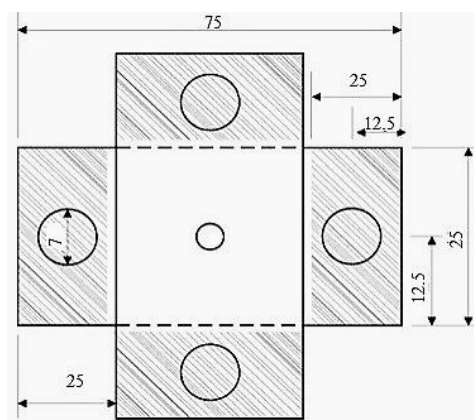
**2.3 Experimental work**

Welding was carried out with the help of a pedestal type inverter-based medium frequency dc machine (Model: PACI TECH-ERSW) of capacity 90 kVA. The machine has the flexibility of welding sheets up to 6 mm thick with a maximum current of 20 kA. The electrode used in the welding consisted of a shank of diameter 16 mm with a conical cap having a tip diameter of 5 mm. The electrode is made up of Cu-Cr-

Zr and is water-cooled during welding. The electrodes are made to hold the sheet specimens under pre-determined pressure, while current is passed through it. The dimension of the steel sheets for both joint is depicted in Figure 2.



**(a) Tensile lap shear Test specimen**



**(b) Cross-tensile test Specimen**

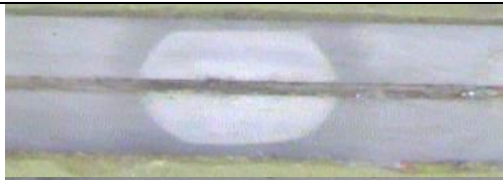


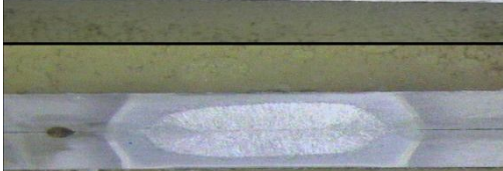


**Fig. 2 Specimen dimension (in mm)**

The resistance spot-welded specimens have been made which are termed as tensile shear fracture load (TSFL) and cross tensile shear fracture load (CTSFL). ASTM guidelines were followed for preparing the test specimens. In order to examine the mechanical properties of the joint, tensile shear test was carried out in 100 KN, servo controlled Universal Testing Machine (Make: FIE-BLUESTAR, INDIA, specimens were etched with freshly prepared 25 ml ethanol, 1.25 ml hydrochloric acid to reveal the microstructures. Specimens were etched with 5% of Nital to reveal the macrostructures. All the joints fabricated in this investigation have been analyzed at low magnification (10×) using stereo zoom optical macroscopic to reveal the quality of RSW regions.

Model: UNITEK 94100). Representative specimens from the as-received steel sheets were cut for microstructural studies in the through-thickness, transverse and longitudinal directions. The specimen blanks were mounted using phenolic resin, ground up to 400-grade emery paper, polished first using 0.6 μm and then using 0.25 μm diamond pastes. The polished

Microstructural analysis was carried out using a light optical microscope (MEIJI-MIL 7100-JAPAN).

**Table 3 Finding the Working Limits of Resistance Spot Welding Parameters**

S.No	Parameter	Range	Figure	Observation
1	Welding Current	<40 kA		Joint was separated
2	Welding Current	>60kA		Metal deformation take place
3	Electrode Force	<3.5 MPa		Less indentation
4	Electrode Force	4.5> MPa		More indentation
5	Welding Time	<0.5 Sec		Tiny defect in center
6	Welding Time	>2.5 Sec		Wider nugget formation

In this investigation for the fabrication of joints the welding current was varied from 40 kA to 60 kA at 5 intervals, similarly, electrode force was varied from 3.5 Mpa to 4.5 MPa at 0.25 interval and welding time 0.5 sec to 2.5 sec at 0.5 intervals. Table 3 shows the finding the working limits of RSW process parameters.

### 3. Results and Discussion

#### 3.1 Developing empirical relationships

In this study, the RSM was used to calculate maximum TSFL and CTSFL of resistance spot welding process parameters can be exposed as,

$$\text{Tensile Shear Fracture Load (TSFL)} = f(C, P, T) \quad (1)$$

$$\text{Cross Tensile Shear Fracture Load (CTSFL)} = f(C, P, T) \quad (2)$$

The selected polynomial Tensile Shear Fracture Load and Cross Tensile Shear Fracture Load of resistance spot welded joints could be conveyed as

$$\text{TSFL} = b_0 + b_1(C) + b_2(P) + b_3(T) + b_{12}(CP) + b_{13}(CT) + b_{23}(PT) - b_{11}(C^2) - b_{22}(P^2) - b_{33}(T^2) \quad (3)$$

$$\text{CTSFL} = b_0 + b_1(C) + b_2(P) + b_3(T) + b_{12}(CP) + b_{13}(CT) + b_{23}(PT) - b_{11}(C^2) - b_{22}(P^2) - b_{33}(T^2) \quad (4)$$

Where  $b_0$  is the average of responses  $b_1, b_2, b_3, \dots, b_{34}$  are the coefficients that depend on respective main and interaction factors [11]. In the above expression, all the factors (main and interaction factors) might not have a huge influence on the responses. The fit summary exposes that the fitted quadratic model is statistically noteworthy to examine the response variables. It is established that the calculated F ratios are bigger than the tabulated values at a 95% confidence level; hence, the models are considered to be adequate [9].

From the ANOVA test results, the important factors were identified, and these factors are included in the final empirical relationships. Thus, developed empirical relationships are given below.

Final equations in terms of the actual factor: -

$$\text{Tensile shear fracture load} = +2.05 + 2.91 * C - 1.45 * P + 0.13 * T - 0.40 * C * P + 0.29 * C * T + 0.094 * C * T + 1.08 * C^2 + 1.06 * P^2 + 0.088 * T^2 \dots \dots \dots (5)$$

$$\text{Cross Tensile shear fracture load} = +2.05 + 2.91 * C - 1.45 * P + 0.13 * T - 0.40 * C * P + 0.29 * C * T + 0.094 * P * T + 1.08 * C^2 + 1.06 * P^2 + 0.088 * T^2 \dots \dots \dots (6)$$

The correlation shows predicted and actual TSFL and CTSFL of resistance spot welding. From the empirical relationship developed, the effect of process parameters on TSFL and CTSFL of resistance spot welded similar joints are obtained. It is clear, that the

strength increments with the expansion of electrode pressure, welding current and welding time to a certain value and afterward diminishes.

#### 3.2 Mechanical Properties

The results for tensile-shear fracture load and cross tensile shear fracture load are presented in Table 4. It is understood that the failure mode is interfacial, and the fracture has initiated from a periphery point and through the weld nugget. Based on the results in the proceeding section, the pointed area has a martensitic microstructure. It is believed that stress concentration due to electrode welding force along the weld nugget periphery results in crack initiation in points which have a martensitic microstructure. As martensite is not a deformable phase, a ductile fracture is not expected. The tensile specimens are failed slightly away from the weld nugget zone (WNZ) i.e., HAZ. The ductility of the weld joints is lower than the base metal. In the present study, the nugget diameter was measured using Image analyzer software and the values are approximately 7.28mm.

**Table 4 Tensile Properties of Welded joints for optimized welding parameters**

S. No	Nugget size measurement (mm)	Tensile shear fracture load (TSFL) kN	Cross tensile shear fracture load (CTSFL) kN
		UTS	UTS
1	7.28	18	15.6

#### 3.3 Microstructural features of the RSW joint

The microstructure of Nugget Zone (NZ), IF and HAZ are illustrated in Figure 3. The NZ and HAZ exhibited a martensitic microstructure and columnar grains in NZ. This is related to the heat cycle of both NZ and HAZ during welding. The high cooling rate of NZ and HAZ after attaining A1 temperature has led to the formation of martensite in these zones.

It is well established by the researchers that the cooling rate of these zones is  $>400^\circ \text{C/s}$  for RSW. The microstructure for 55 kA depicts regular martensite at the middle of the NZ and away from NZ, it shows two regions of the heat affected zone upper critical (UC) and sub-critical (SC) HAZ.



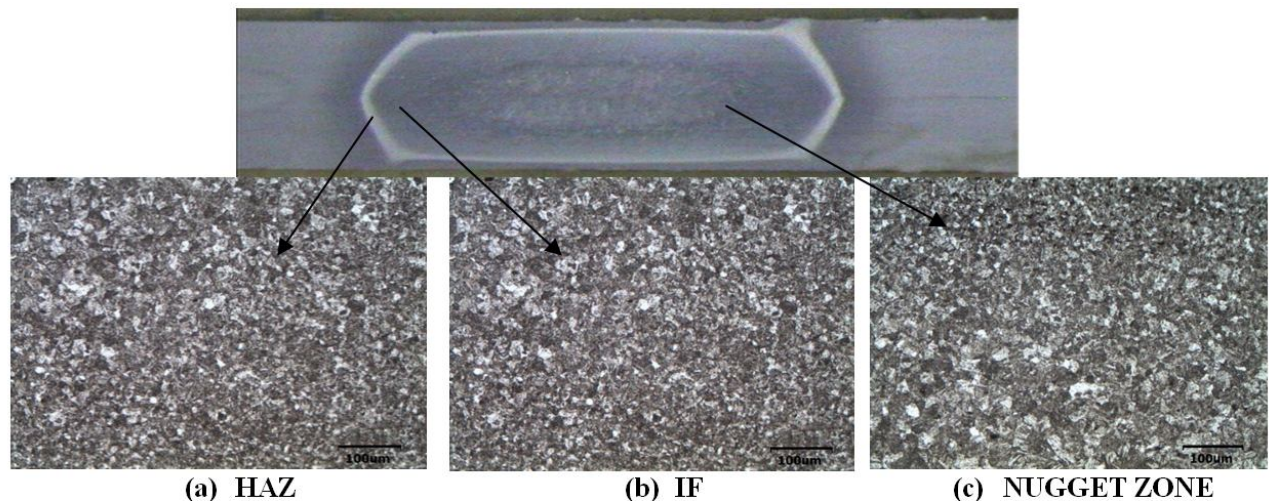


Fig. 3 Microstructural features of optimized joint

#### 4. Conclusions

- The welding current is the major influencing parameter compared to other parameters such as electrode force and welding time.
- The resistance spot welding process parameters were optimized using response optimization to get the maximum strength tensile shear fracture load and cross tensile shear fracture load.
- The maximum strength of tensile shear fracture load and cross tensile shear fracture loads such as 18 and 15.26 kN achieved under welding current 55 kA, electrode pressure 4 MPa and welding time 2 sec.
- Nugget interfacial failure mode was observed in fractured specimens, where the initial cracks were initiated from the periphery point and through the weld region.

#### References

1. Mucha J, Kaščák L and Spišák E (2013), "The experimental analysis of forming and strength of Clinch Riveting sheet metal joint made of different materials", *Adv.Mech. Eng.*, Vol. 59, 1-11.
2. Zhang X, Chen G, Zhang Y and Lai X (2009), "Improvement of resistance spot weldability for dual-phase (DP600) steels using servo gun", *J. Mat. Proc. Technol.*, Vol. 209, 2671-2675.
3. Hernandez V H B, Panda S K, Okita Y and Zhou N Y (2010), "A study on heat affected zone softening in resistance spot welded dual phase steel by nanoindentation", *J. Mat. Sci.*, Vol. 45, 1638-1647.
4. Kaščák L, Brezinová J, Mucha J (2015), "Evaluation of corrosion resistance of galvanized steel sheets used in automotive production", *Mat. Sci. Forum*, Vol. 818, 141-144.
5. Dancette S, Fabregue D, Estevez R, Massardier V, Dupuy T and Bouzekri M (2012), "A finite element model for the prediction of Advanced High Strength Steel spot welds fracture", *Eng. Fracture Mech.*, Vol.87, 48-61.
6. Kaščák L, Spišák E and Gajdoš I (2015), "Influence of welding parameters on the quality of resistance spot welded joints of DP600 steels", *Key Eng. Mat.*, Vol. 635, 143-146.
7. Pouranvari M, Marashi S P H and Jaber H L (2015), "DP780 dual-phase-steel spot welds: critical fusion-zone size ensuring the pull-out failure mode", *Mat. Technol.*, Vol. 49, 579-585.
8. Lifang M, Jiming Y, Dongbing Y, Jinwu L and Genyu C (2012), "Comparative study on CO2 laser overlap welding and resistance spot welding for galvanized steel", *Mat.Design*, Vol. 40, 433-442.
9. S J Hu, J Senkara and H Zhang: quality definition of resistance spot welds: A structural point of view, in proceeding of international body engineering conference IBEC'96, body and engineering section, Detroit, MI 1996